Supporting information for article:

N-Iodosaccharin–pyridine co-crystal system under pressure: experimental evidence of reversible twinning

Vishnu Vijayakumar-Syamala, Emmanuel Aubert, Maxime Deutsch, Emmanuel Wenger, Arun Dhaka, Marc Fourmigué, Massimo Nespolo and Enrique Espinosa

N-iodosaccharin-pyridine co-crystal system under pressure: experimental evidence of reversible twinning

Vishnu Vijayakumar-Syamala[1], Emmanuel Aubert[1], Maxime Deutsch,[1] Emmanuel Wenger[1], Arun Dhaka[2], Marc Fourmigué[2], Massimo Nespolo[1], Enrique Espinosa[1]

[1]Université de Lorraine, CNRS, CRM2, Nancy, France. [2]Univ Rennes, CNRS, ISCR (Institut des Sciences Chimiques de Rennes) UMR 6226, Rennes 35042, France. *enrique.espinosa@univ-lorraine.fr*

Supplementary Information

SI.1. Synthesis and co-crystallization

NISac was prepared as previously reported (Dolenc, 2000). Pyridine (99% from Alfa Aesar) was commercially available and used as received. A 1:1 stoichiometric co-crystal of N-iodosaccharin and pyridine (*NISac·Py*) was prepared by dissolving 5 mg of N-iodosaccharin (0.016 mmol) in 1 mL of ethyl acetate inside a 5ml glass vial, stirred and gently heated in a hot-plate. Pyridine (0.002 mL, 0.02 mmol) was added slowly to the solution and the mixture was further heated and stirred for another 10 minutes until obtaining a clear saturated solution. The vial was covered with aluminium foil for reducing any damage that can be caused by light or air, kept in a dark place for slow solvent evaporation. Colourless, thin, plat crystals were obtained after two days.

SI.2. Crystal choice

Crystals grown from ethyl acetate had a similar thin plate morphology but with different crystal habits, making important the choice of the crystals for the high-pressure X-ray diffraction investigation. Crystals were selected using a polarized light microscope. A first type of crystals (Figure SI-2a) show two distinct colours separated by a line, on the large face of the crystal, suggesting the sample may be twinned. Initial unit cell determination on such crystals shows the presence of different orientations for the reciprocal lattice, confirming their twinning. On the other hand, crystals of second type (Figure SI-2b) show a homogeneous

colour across the surface when observed under the polarized light microscope, except for the edges. Such a difference may however be caused by changes in thickness. The diffraction pattern of these crystals could be indexed at 100% with a single orientation of the reciprocal lattice, excluding at least non-merohedric twinning. These crystals were chosen for crystal structure determination at room- and high-pressures.

SI.3. Membrane Diamond Anvil Cell loading

A Le Toullec-type Membrane Diamond Anvil Cell (MDAC) with a small height and a large opening angle of 100°, designed by BETSA company, was chosen for the high-pressure X-ray diffraction experiments. This large opening angle serves the purpose of accessing a larger proportion of the reciprocal space. The MDAC is equipped with type IIa diamonds with a cullet size of 600 μm; the sample chamber is a hole of 280 μm in diameter, which is drilled at the centre of a stainless-steel gasket with an initial thickness of 200 μm pre-indented to a thickness of 90 μm. The sample is loaded inside the MDAC chamber along with a ruby sphere of ~10μm in diameter for in-situ measurement of pressure by ruby luminescence (PRL) technique (Piermarini *et al.*, 1975). A Labview program, developed on AILES beamline at SOLEIL synchrotron (Voute *et al.*, 2016) was used to measure the pressure inside the MDAC. The whole PRL set-up is installed on the top of an anodized aluminium rail that is fixed directly on the base of the goniometer, which allows it to move backwards during data collection and forwards during pressure calibration (Figure SI-2c). The use of the adjustable stops and the clamping screws allows the PRL to be repositioned very precisely.

Table SI-1 Crystallographic information for data collected at ambient conditions with crystal-1

Crystal data	
Chemical formula	$C_{12}H_9IN_2O_3S$
M_r	388.17
Crystal system, space group	Monoclinic, $B2_1/e$
Temperature (K)	293
a, b, c (Å)	27.234 (3), 7.8058 (7), 12.6258 (10)
β (°)	88.606 (2)
V (Å^3)	2683.2 (4)
Z	8
Radiation type	Mo $K\alpha$ (λ=0.7107 Å)
μ (mm^{-1})	2.55
Crystal size (mm)	0.149 × 0.122 × 0.053
Data collection	
Diffractometer	Bruker D8 Venture
Absorption correction	Numerical (face indexing)
No. of measured, independent and observed [$I > 2\sigma(I)$] reflections	109428, 3759, 3456
R_{int}	0.034
$(\sin\theta/\lambda)_{max}$ (Å^{-1})	0.694
Refinement	
$R[F^2 > 2\sigma(F^2)]$, $wR(F^2)$, S	0.019, 0.050, 1.09
No. of reflections	3759
No. of parameters	173
H-atom treatment	H-atom parameters constrained
$\Delta\rho_{max}$, $\Delta\rho_{min}$ (e Å^{-3})	0.73, -0.29

Table SI-2 Crystallographic information for data collected at ambient conditions with crystal-2.

Crystal data	
Chemical formula	$C_{12}H_9IN_2O_3S$
M_r	388.17
Crystal system, space group	Monoclinic, $B2_1/e$
Temperature (K)	293
a, b, c (Å)	27.272 (5), 7.8156 (9), 12.6155 (16)
β (°)	88.703 (3)
V (Å^3)	2688.3 (7)
Z	8
Radiation type	Mo $K\alpha$ (λ=0.7107 Å)
μ (mm^{-1})	2.54
Crystal size (mm)	0.110 × 0.091 × 0.048
Data collection	
Diffractometer	Bruker APEX-II CCD
Absorption correction	Numerical (face indexing)
No. of measured, independent and observed [I >2σ(I)] reflections	67239, 2738, 2670
R_{int}	0.049
$(\sin\theta/\lambda)_{max}$ (Å^{-1})	0.625
Refinement	
$R[F^2 > 2\sigma(F^2)]$, $wR(F^2)$, S	0.063, 0.155, 1.16
No. of reflections	2738
No. of parameters	173
H-atom treatment	H-atom parameters constrained
$\Delta\rho_{max}$, $\Delta\rho_{min}$ (e Å^{-3})	2.49, -1.41

Table SI-3 Unit cell parameters and volume as a function of the pressure for the *NISac·Py* DFT optimized crystal structures (*B*2$_1$/*e* setting of the space group). Unit cell void volume and percentage were calculated with ASV program.

P (GPa)	*a*(Å)	*b*(Å)	*c*(Å)	*β*(°)	*V*(Å$_3$)	Void(Å^3)	% Void
-0.25	27.0687	7.8280	12.6586	88.21	2680.95	771.91	28.79
0.00	26.9932	7.7202	12.6043	88.49	2625.75	718.78	27.37
0.25	26.9098	7.5636	12.5304	88.63	2549.64	644.67	25.28
0.50	26.8129	7.4921	12.4737	88.85	2505.27	602.15	24.04
0.75	26.6909	7.4129	12.4300	88.85	2458.85	557.54	22.67
1.00	26.6453	7.3484	12.3971	88.98	2426.96	527.45	21.73
1.25	26.5475	7.2755	12.3599	88.99	2386.89	488.86	20.48
1.50	26.4287	7.2398	12.2916	89.09	2351.57	455.34	19.36
1.75	26.3958	7.1942	12.2782	89.24	2331.38	436.73	18.73
2.00	26.3438	7.1548	12.2371	89.17	2306.28	412.94	17.91
2.25	26.3334	7.1196	12.1568	89.42	2279.09	387.54	17.00
2.50	26.2937	7.0845	12.1322	89.50	2259.87	369.74	16.36
2.75	26.2385	7.0497	12.1099	89.65	2239.96	351.35	15.69
3.00	26.1848	7.0276	12.0759	89.66	2222.13	334.79	15.07
3.25	26.1447	7.0038	12.0309	89.72	2202.96	316.94	14.39
3.50	26.1034	6.9773	12.0308	89.87	2191.17	306.72	14.00
3.75	26.0893	6.9539	11.9751	89.97	2172.53	289.20	13.31
4.00	26.0743	6.9255	11.9585	90.00	2159.44	277.48	12.85
4.25	26.0102	6.9094	11.9316	90.12	2144.30	263.61	12.29
4.50	25.9742	6.8825	11.9113	90.17	2129.35	250.07	11.74
4.75	25.9571	6.8586	11.8996	90.18	2118.46	240.62	11.36
5.00	25.9165	6.8424	11.8590	90.29	2102.95	226.25	10.76
5.25	25.8982	6.8307	11.7979	90.53	2086.98	211.27	10.12
5.50	25.8896	6.8063	11.7820	90.54	2076.04	201.50	9.71
5.75	25.8736	6.7883	11.7616	90.61	2065.66	192.41	9.31
6.00	25.8562	6.7735	11.7314	90.74	2054.44	182.32	8.87

Table SI-4 Bader's atomic charges (B3LYP-D3 Def2TZVPP) in *NISac.Py* isolated adduct and in NISac and Py isolated molecules extracted from the structure at ambient conditions.

	NISac·Py	NISac	Py
Atom label	**Q (|e|)**	**Q (|e|)**	**Q (|e|)**
I1	0.48	0.42	
N1	-1.36	-1.29	
S1	3.15	3.15	
O1	-1.36	-1.35	
O2	-1.35	-1.33	
O3	-1.17	-1.14	
C1	0.02	0.03	
H1	0.05	0.06	
C2	0.01	0.02	
H2	0.02	0.03	
C3	0.01	0.02	
H3	0.02	0.03	
C4	0.03	0.04	
H4	0.05	0.06	
C5	-0.18	-0.17	
C6	0.00	0.01	
C7	1.42	1.42	
N2	-1.20		-1.13
C8	0.54		0.55
H8	0.07		0.02
C9	0.01		-0.02
H9	0.05		0.01
C10	0.02		0.00
H10	0.04		0.02
C11	0.02		-0.01
H11	0.05		0.01
C12	0.51		0.52
H12	0.08		0.03

Table SI-5 Crystallographic information for crystal-1 at 100K.

Crystal data	
Chemical formula	$C_{12}H_9IN_2O_3S$
M_r	388.17
Crystal system, space group	Monoclinic, $B2_1/e$
Temperature (K)	100
a, b, c (Å)	27.085 (5), 7.6524 (9), 12.5325 (14)
β (°)	88.571 (2)
V (Å^3)	2596.7 (6)
Z	8
Radiation type	Mo $K\alpha$ (λ=0.7107 Å)
μ (mm^{-1})	2.63
Crystal size (mm)	0.149 × 0.122 × 0.053
Data collection	
Diffractometer	Bruker APEX-II CCD
Absorption correction	Numerical (face indexing)
No. of measured, independent and observed [I >2σ(I)] reflections	104622, 3643, 3587
R_{int}	0.031
$(\sin\theta/\lambda)_{max}$ (Å^{-1})	0.694
Refinement	
$R[F^2 > 2\sigma(F^2)]$, $wR(F^2)$, S	0.015, 0.038, 1.13
No. of reflections	3643
No. of parameters	173
H-atom treatment	H-atom parameters constrained
$\Delta\rho_{max}$, $\Delta\rho_{min}$ (e Å^{-3})	1.04, -0.32

Table SI-6 Principal compressibilities and corresponding principal axes of compression obtained from the high-pressure data-sets of *NISac.Py*. X_i – Principal axis of compressibility, K_i – principal compressibility value and σK_i – standard deviation of principal compressibility value. Experimental/ theoretical results are shown as left/right values.

Principal axis, X_i	K_i (TPa^{-1})	σK_i (TPa^{-1})	Components of X_i along the crystallographic axes		
			a	b	c
1	26.9927/18.8562	1.6427/0.8223	0.0000/0.0000	-1.0000/-1.0000	0.0000/0.0000
2	15.2596/12.4827	0.9622/0.2187	0.3432/0.2469	0.0000/0.0000	0.9393/0.9691
3	9.0744/ 5.7314	0.387 /0.3329	0.5013/0.6369	0.0000/0.0000	-0.8653/-0.7709

Table SI-7 CrystalExplorer decomposition of total interactions energy (E_tot) in electrostatic (E_ele), polarization (E_pol), dispersion (E_dis) and repulsion (E_rep) terms of the *NISac·Py*. Sym. Op denotes the symmetry operation of the adduct interacting with the reference *x,y,z* adduct (R is the intermolecular centroid to centroid distance). All energies are given in kJ/mol.

Sym. Op.	R (Å)	E_ele	E_pol	E_dis	E_rep	E_tot
½-*x*,-½+*y*,1-*z* [a]	5.74	-60.2	-6.8	-51.5	37.6	-80.9
½-*x*,1-*y*,1.5-*z* [a]	8.59	-60.5	-11.9	-29.7	22.7	-79.4
1-*x*,1-*y*,1-*z*	9.75	-23.1	-5.4	-12.7	14.1	-27.2
½-*x*,1-*y*,½-*z* [a]	6.53	-10.1	-7.9	-23.4	15.7	-25.9
x,½-*y*,-½+*z* [a]	7.01	-7.7	-8.1	-16.9	10.2	-22.6
1-*x*,-½+*y*,½-*z*	11.39	-12.7	-1.9	-17.4	9.7	-22.3
$\overline{½}$+*x*,*y*,½+*z*	14.87	0.3	-1.3	-6.4	2.5	-4.8
1-*x*,1-*y*,-*z*	14.66	-1.4	-0.3	-4.9	1.9	-4.6
x,1.5-*y*,$\overline{½}$+*z* [a]	7.9	6.6	-2.6	-7.9	3.2	-0.9
[a] interactions ensuring cohesion of (200) molecular planes						

Table SI-8 N_{sac}-I1···N'$_{py}$ XB distances and angle, and angle between the molecular planes, determined from the experimental high-pressure data-sets of *NISac.Py. The a*ngle between molecular planes was calculated using the MPLA option in Olex2-1.3.

Pressure (GPa)	0.00(5)	0.00(5)	0.05(5)	0.20(5)	0.4(1)	0.5(1)	0.5(1)	0.8(1)	0.9(1)	1.3(2)	1.5(2)	1.9(2)	2.0(2)	2.4(2)	3.3(2)	4.5(2)
Nsac-I1 (Å)	2.240(16)	2.23(2)	2.21(2)	2.231(18)	2.21(2)	2.214(18)	2.231(19)	2.233(19)	2.220(18)	2.22(2)	2.23(2)	2.25(2)	2.26(3)	2.26(2)	2.248(11)	2.249(16)
I1···N'Py (Å)	2.295(13)	2.252(18)	2.258(18)	2.26(15)	2.256(18)	2.235(15)	2.245(16)	2.219(16)	2.203(15)	2.192(19)	2.181(17)	2.17(2)	2.14(2)	2.168(19)	2.218(9)	2.162(13)
Nsac···N'Py (Å)	4.53(2)	4.48(3)	4.46(3)	4.49(2)	4.46(3)	4.44(2)	4.47(3)	4.45(2)	4.42(2)	4.40(3)	4.40(3)	4.41(3)	4.39(3)	4.42(3)	4.457(13)	4.400(18)
(Nsac-I1)/ (Nsac···N'Py)	0.494(4)	0.498(6)	0.496(6)	0.497(5)	0.496(6)	0.499(5)	0.499(5)	0.502(5)	0.502(5)	0.505(6)	0.507(6)	0.510(6)	0.515(8)	0.511(6)	0.504(3)	0.511(4)
(I1···N'Py)/ (Nsac···N'Py)	0.507(4)	0.503(5)	0.506(5)	0.503(4)	0.506(5)	0.503(4)	0.502(5)	0.499(4)	0.498(4)	0.498(5)	0.496(5)	0.492(6)	0.487(6)	0.490(5)	0.498(2)	0.491(4)
Nsac-I1···N'Py (°)	174.5(3)	174.1(5)	174.6(5)	174.4(4)	174.5(5)	174.3(4)	173.9(5)	173.7(5)	173.5(4)	173.3(6)	172.9(5)	172.2(6)	171.9(7)	172.3(6)	172.8(8)	172.0(4)
Angle between molecular planes(°)	41.729 (217)	42.388 (312)	41.773 (300)	42.132 (260)	41.547 (285)	41.594 (245)	41.820 (266)	41.990 (269)	41.450 (244)	42.064 (331)	41.582 (282)	41.648 (335)	42.082 (347)	41.649 (298)	41.629 (146)	42.620 (211)

Table SI-9 Nsac-I1···N'py XB distances and angle, and angle between the molecular planes, determined from the theoretical high-pressure data-sets of *NISac.Py. The a*ngle between molecular planes was calculated using Mercury (version 2020.1).

Pressure (GPa)	-0.03	0.22	0.47	0.72	0.97	1.22	1.47	1.72	1.97	2.22	2.47	2.72	2.97	3.22	3.47	3.72	3.97	4.22	4.47	4.72
Nsac-I1 (Å)	2.273	2.276	2.274	2.272	2.275	2.274	2.273	2.274	2.271	2.271	2.271	2.271	2.269	2.269	2.269	2.265	2.266	2.265	2.264	2.263
I1-N'Py (Å)	2.303	2.292	2.287	2.283	2.276	2.271	2.269	2.265	2.261	2.261	2.253	2.252	2.248	2.248	2.245	2.241	2.240	2.237	2.237	2.236
Nsac-N'Py (Å)	4.570	4.563	4.556	4.549	4.545	4.540	4.536	4.532	4.525	4.525	4.516	4.514	4.508	4.508	4.505	4.497	4.496	4.492	4.491	4.488
(Nsac-I1)/ (Nsac-N'Py)	0.497	0.499	0.499	0.499	0.501	0.501	0.501	0.502	0.502	0.502	0.503	0.503	0.503	0.503	0.504	0.504	0.504	0.504	0.504	0.504
(I1-N'Py)/ (Nsac-N'Py)	0.504	0.502	0.502	0.502	0.501	0.500	0.500	0.500	0.500	0.500	0.499	0.499	0.499	0.499	0.498	0.498	0.498	0.498	0.498	0.498
Nsac-I1-N'Py (°)	174.4	174.7	174.5	174.4	174.2	174.4	174.0	173.6	173.7	173.4	172.9	172.9	172.8	172.8	172.6	172.7	172.4	172.5	172.4	172.4
Angle between molecular planes(°)	42.42	42.06	41.63	41.42	41.01	40.78	40.68	41.73	41.02	41.36	42.20	42.10	42.11	42.21	42.53	42.18	42.86	42.73	43.00	42.92

Table SI-10 Variation of intermolecular distances and angles involving I1(x,y,z) and atoms of neighbouring molecules as a function of pressure for the experimental data-sets. Values within brackets are the standard deviations of the corresponding distances. Distance and reduction ratio (RR) are shown as left/right values. RR is defined as the ratio between the internuclear distance and the sum of van der Waals radii of interacting atoms. The rank based on minimum RR is sorted from smaller to larger RR values at 4.5(2) GPa. Δ(RR) is calculated as the difference between maximum and minimum RR values. The distances are given in Å and the angles are given in degrees (°).

Pressure (GPa)	1/2-X,-1/2+Y,1-Z					1/2-X,1-Y,1.5-Z			X,1/2-Y,1/2+Z	1/2-X,1/2+Y,1-Z			
	I1···C8/ RR	I1···I1/ RR	I1···N2/ RR	I1···H8/ RR	<I1···H8-C8	I1···C11/ RR	I1···H11/ RR	<I1···H1-C11	I1···O3/ RR	I1···C12/ RR	I1···N2/ RR	I1···H12/ RR	<I1···H12-C12
0.00(5)	3.671(9)/1.00	4.3683(14)/1.10	4.097(7)/1.16	3.39/1.07	96.0	4.024(9)/1.09	3.46/1.09	113.9	4.016(8)/1.15	3.938(8)/1.07	3.912(7)/1.11	3.88/1.22	85.4
0.00(5)	3.671(14)/1.00	4.372(2)/1.10	4.119(10)/1.17	3.35/1.05	98.4	4.028(14)/1.09	3.47/1.09	112.9	4.031(11)/1.15	3.935(12)/1.07	3.901(10)/1.11	3.88/1.22	85.1
0.05(5)	3.666(13)/1.00	4.362(2)/1.10	4.111(10)/1.16	3.35/1.05	98.0	4.023(13)/1.09	3.48/1.09	112.3	4.012(11)/1.15	3.948(11)/1.07	3.892(10)/1.10	3.92/1.23	83.8
0.20(5)	3.632(11)/0.99	4.3149(17)/1.09	4.063(8)/1.15	3.35/1.05	96.2	4.003(11)/1.09	3.45/1.08	113.3	3.979(9)/1.14	3.913(10)/1.06	3.865(8)/1.09	3.85/1.21	85.0
0.4(1)	3.613(13)/0.98	4.2589(19)/1.08	4.012(10)/1.14	3.35/1.05	94.8	3.957(13)/1.08	3.37/1.06	115.2	3.950(11)/1.13	3.882(10)/1.05	3.831(9)/1.09	3.81/1.20	85.6
0.5(1)	3.599(11)/0.98	4.2145(15)/1.06	3.976(8)/1.13	3.38/1.06	92.6	3.932(11)/1.07	3.36/1.06	113.9	3.91(1)/1.12	3.87(9)/1.05	3.793(8)/1.07	3.84/1.21	83.3
0.5(1)	3.603(12)/0.98	4.2358(18)/1.07	4.010(9)/1.14	3.32/1.04	96.1	3.950(12)/1.07	3.39/1.07	113.6	3.926(10)/1.12	3.871(10)/1.05	3.801(9)/1.08	3.82/1.20	84.3
0.8(1)	3.555(12)/0.97	4.1529(17)/1.05	3.941(9)/1.12	3.29/1.03	95.2	3.897(13)/1.06	3.31/1.04	115.0	3.865(11)/1.10	3.823(10)/1.04	3.740(9)/1.06	3.77/1.19	84.3
0.9(1)	3.543(11)/0.96	4.120(15)/1.04	3.899(8)/1.10	3.3/1.04	93.6	3.853(12)/1.05	3.25/1.02	116.0	3.851(10)/1.10	3.808(9)/1.03	3.729(8)/1.06	3.76/1.18	84.4
1.3(2)	3.501(16)/0.95	4.079(2)/1.03	3.864(12)/1.09	3.26/1.03	93.8	3.822(15)/1.04	3.20/1.01	117.3	3.808(13)/1.09	3.784(13)/1.03	3.703(11)/1.05	3.71/1.17	85.3
1.5(2)	3.485(14)/0.95	4.0421(18)/1.02	3.836(10)/1.09	3.23/1.02	94.4	3.799(13)/1.03	3.17/1.00	117.1	3.782(11)/1.08	3.767(11)/1.02	3.672(10)/1.04	3.72/1.17	84.3
1.9(2)	3.430(16)/0.93	3.993(2)/1.01	3.786(12)/1.07	3.14/0.99	96.4	3.760(15)/1.02	3.14/0.99	117.0	3.724(13)/1.06	3.725(13)/1.01	3.647(12)/1.03	3.64/1.14	86.0
2.0(2)	3.431(16)/0.93	3.984(2)/1.01	3.782(12)/1.07	3.15/0.99	95.9	3.748(16)/1.02	3.10/0.97	119.0	3.712(14)/1.06	3.717(13)/1.01	3.630(12)/1.03	3.61/1.14	87.3
2.4(2)	3.413(14)/0.93	3.947(2)/1.00	3.744(11)/1.06	3.11/0.98	96.6	3.738(14)/1.02	3.11/0.98	117.1	3.676(12)/1.05	3.694(11)/1.00	3.613(11)/1.02	3.59/1.13	86.8
3.3(2)	3.386(8)/0.92	3.8644(11)/0.98	3.691(5)/1.05	3.12/0.98	94.6	3.690(7)/1.00	3.11/0.98	113.9	3.603(6)/1.03	3.641(5)/0.99	3.562(5)/1.01	3.59/1.13	83.7
4.5(2)	3.350(11)/0.91	3.7902(15)/0.96	3.641(8)/1.03	3.06/0.96	95.6	3.643(10)/0.99	3.07/0.97	113.3	3.533(8)/1.01	3.602(8)/0.98	3.530(8)/1.00	3.53/1.11	85.2
Rank based on minimum RR	1	2	9	3	-	6	4	-	8	5	7	10	-
Δ(RR)	0.09	0.14	0.13	0.11	-	0.10	0.12	-	0.14	0.09	0.11	0.11	-

Table SI-11   Variation of intermolecular distances and angles involving I1(x,y,z) and atoms of neighbouring molecules as a function of pressure for the theoretical data-sets. Values within brackets are the standard deviations of the corresponding distances. Distance and reduction ratio (RR) are shown as left/right values. RR is defined as the ratio between the internuclear distance and the sum of van der Waals radii of interacting atoms. The rank based on minimum RR is sorted from smaller to larger RR values at 4.5(2) GPa. Δ(RR) is calculated as the difference between maximum and minimum RR values. The distances are given in Å and the angles are given in degree (°).

Pressure[a] (GPa)	1/2-X,-1/2+Y,1-Z					1/2-X,1-Y,1.5-Z			X,1/2-Y,1/2+Z	1/2-X,1/2+Y,1-Z			
	I1···C8/ RR	I1···I1/ RR	I1···N2/ RR	I1···H8/ RR	<I1···H8-C8	I1···C11/ RR	I1···H11/ RR	<I1···H1-C11	I1···O3/ RR	I1···C12/ RR	I1···N2/ RR	I1···H12/ RR	<I1···H12-C12
-0.03	3.658/0.99	4.336/1.09	4.087/1.16	3.35/1.05	97.7	4.059/1.10	3.50/1.10	113.5	4.003/1.14	3.928/1.07	3.913/1.11	3.82/1.20	87.7
0.22	3.602/0.98	4.284/1.08	4.026/1.14	3.30/1.04	97.2	4.055/1.10	3.51/1.10	112.9	3.966/1.13	3.865/1.05	3.859/1.09	3.75/1.18	87.7
0.47	3.553/0.97	4.200/1.06	3.955/1.12	3.26/1.02	96.5	3.965/1.08	3.40/1.07	113.8	3.891/1.11	3.833/1.04	3.789/1.07	3.74/1.18	86.7
0.72	3.529/0.96	4.160/1.05	3.920/1.11	3.24/1.02	96.0	3.922/1.07	3.35/1.05	113.9	3.841/1.10	3.816/1.04	3.758/1.06	3.73/1.17	86.3
0.97	3.504/0.95	4.110/1.04	3.882/1.10	3.22/1.01	96.8	3.877/1.05	3.30/1.04	114.1	3.790/1.08	3.810/1.04	3.729/1.06	3.73/1.17	85.9
1.22	3.479/0.95	4.077/1.03	3.850/1.09	3.20/1.01	95.5	3.852/1.05	3.28/1.03	114.1	3.760/1.07	3.788/1.03	3.699/1.05	3.71/1.17	85.7
1.47	3.470/0.94	4.030/1.02	3.824/1.08	3.20/1.01	94.8	3.799/1.03	3.21/1.01	114.8	3.721/1.06	3.779/1.03	3.665/1.04	3.71/1.17	85.4
1.72	3.448/0.94	3.996/1.01	3.792/1.07	3.19/1.00	94.3	3.781/1.03	3.19/1.00	114.9	3.684/1.05	3.759/1.02	3.655/1.04	3.67/1.15	86.4
1.97	3.432/0.93	3.978/1.00	3.755/1.06	3.18/1.00	94.2	3.760/1.02	3.17/1.00	114.8	3.662/1.05	3.753/1.02	3.633/1.03	3.68/1.16	85.5
2.22	3.420/0.93	3.949/1.00	3.754/1.06	3.17/1.00	93.9	3.734/1.01	3.14/0.99	114.9	3.639/1.04	3.741/1.02	3.618/1.02	3.66/1.15	85.9
2.47	3.398/0.92	3.920/0.99	3.723/1.05	3.16/0.99	93.2	3.734/1.01	3.15/0.99	114.6	3.632/1.04	3.682/1.00	3.594/1.02	3.57/1.12	87.3
2.72	3.384/0.92	3.902/0.99	3.704/1.05	3.15/0.99	93.0	3.717/1.01	3.13/0.98	114.6	3.613/1.03	3.670/1.00	3.579/1.01	3.56/1.12	87.2
2.97	3.370/0.92	3.879/0.98	3.688/1.04	3.13/0.98	93.0	3.696/1.00	3.11/0.98	114.3	3.587/1.02	3.663/1.00	3.566/1.01	3.55/1.12	87.2
3.22	3.363/0.91	3.865/0.98	3.675/1.04	3.13/0.98	93.0	3.677/1.00	3.10/0.97	114.2	3.571/1.02	3.656/0.99	3.559/1.01	3.54/1.11	87.2
3.47	3.352/0.91	3.848/0.97	3.662/1.04	3.11/0.98	93.0	3.655/0.99	3.08/0.97	113.7	3.554/1.02	3.642/0.99	3.550/1.01	3.52/1.11	87.5
3.72	3.341/0.91	3.835/0.97	3.650/1.03	3.11/0.98	92.7	3.648/0.99	3.07/0.97	113.8	3.533/1.01	3.642/0.99	3.539/1.00	3.53/1.11	87.1
3.97	3.329/0.90	3.817/0.96	3.636/1.03	3.09/0.97	92.9	3.636/0.99	3.07/0.97	113.0	3.525/1.01	3.609/0.98	3.526/1.00	3.48/1.09	87.8
4.22	3.318/0.90	3.803/0.96	3.623/1.03	3.08/0.97	92.7	3.624/0.98	3.06/0.96	112.9	3.513/1.00	3.598/0.98	3.512/0.99	3.47/1.09	87.7
4.47	3.313/0.90	3.789/0.96	3.613/1.02	3.08/0.97	92.7	3.610/0.98	3.05/0.96	112.9	3.487/1.00	3.595/0.98	3.509/0.99	3.47/1.09	87.8
4.72	3.303/0.90	3.777/0.95	3.601/1.02	3.07/0.97	92.5	3.599/0.98	3.04/0.95	112.8	3.473/0.99	3.584/0.97	3.495/0.99	3.46/1.09	87.6
Rank based on minimum RR	1	2	9	4	-	6	3	-	8	5	7	10	-
Δ(RR)	0.09	0.14	0.14	0.08	-	0.12	0.15	-	0.15	0.10	0.12	0.11	-

[a] The pressure values given here are corrected based on the hypothesis discussed in section 6.1.
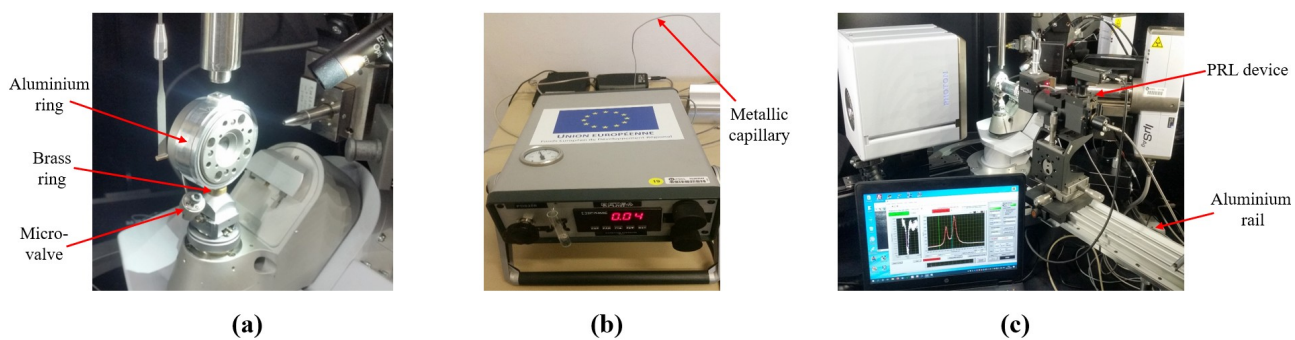
Figure SI-1 (a) In-house developed goniometer head used for the HPXRD experiments. Aluminium ring to hold the cell, brass ring used to strengthen the Z-stage of the goniometer head and micro-valve that is used to connect the pneumatic drive system to the MDAC (the screw on top can be used to open or close the valve) are highlighted, (b) Pneumatic drive system used to apply force on the diamonds. The capillary that connects the pneumatic drive system to the micro-valve of MDAC is highlighted, (c) MDAC installed in the diffractometer chamber along with the PRL device, which can be moved back and forth through the aluminium rail attached to the goniometer base.
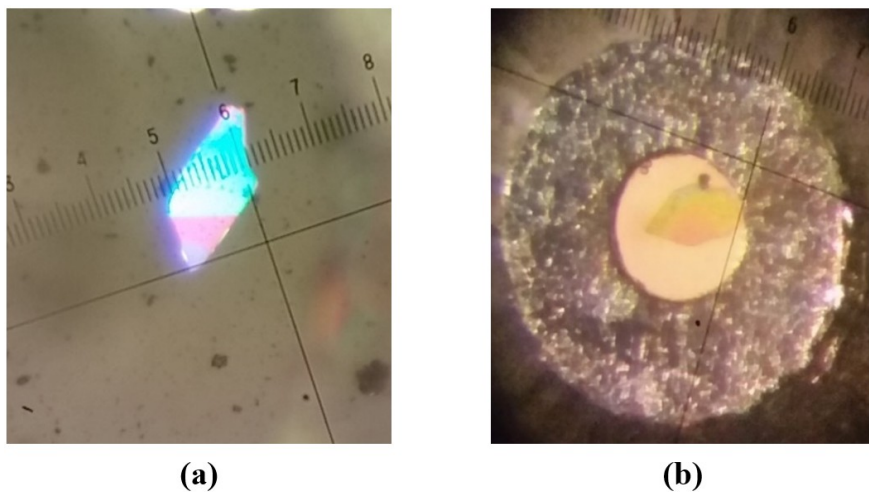
Figure SI-2 *NISac·Py* crystals showing different crystal habits: (a) two distinct colours are observed on the surface separated by a line, (b) a homogenous colour is observed on the surface except for the edges.

(0*kl***)* plane**

Zoomed portion of (0*kl***)* plane**

3D profile of the indicated peak

(*h***0***l***)* plane**

Zoomed portion of (*h***0***l***)* plane**

3D profile of the indicated peak
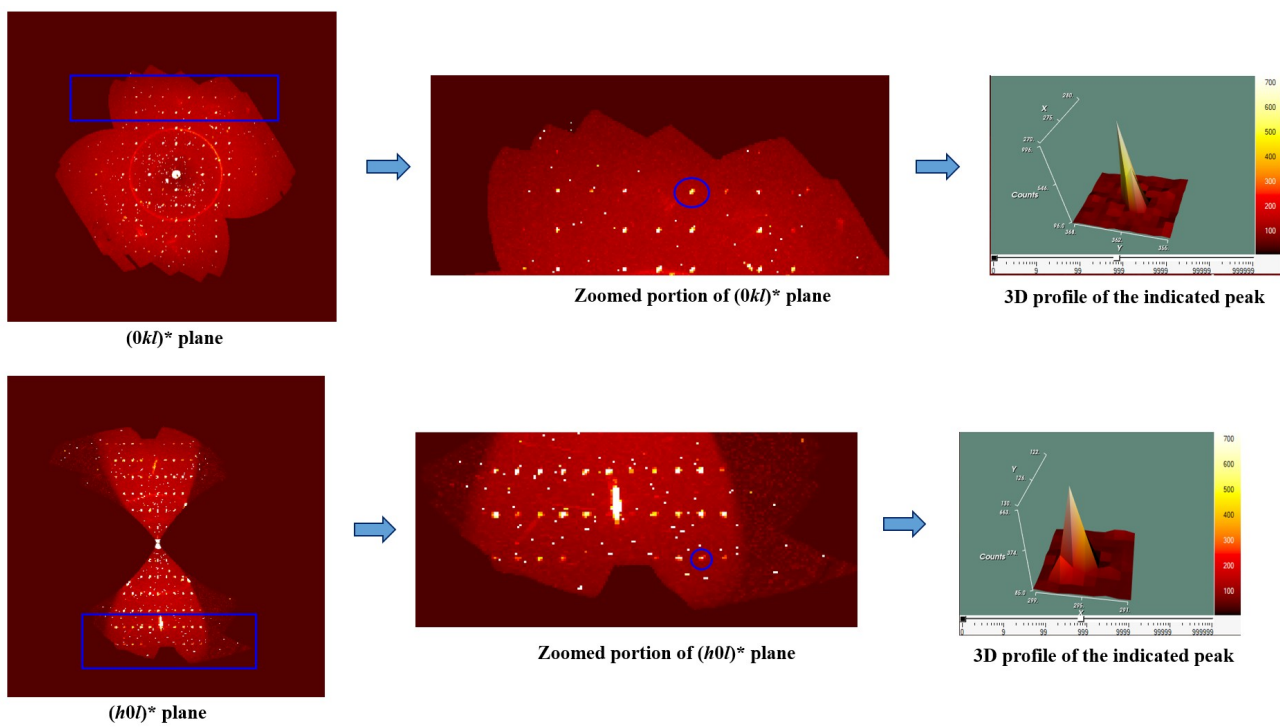
Figure SI-3 Reconstruction of selected reciprocal lattice planes (0kl)* and (h0l)* based on the X-ray diffraction data at 3.3(2) GPa. In addition to the diffraction peaks coming from the sample, the frames also contain those coming from diamonds and ruby, and hot pixels (of high intensity). The 3D profile of the selected peaks do not show any splitting, indicating that reflections issued from both domains overlap to each other.

**Diffraction frames with
a reflection highlighted**

**Zoomed portion of
highlighted reflection**

3D profile of the highlighted reflection
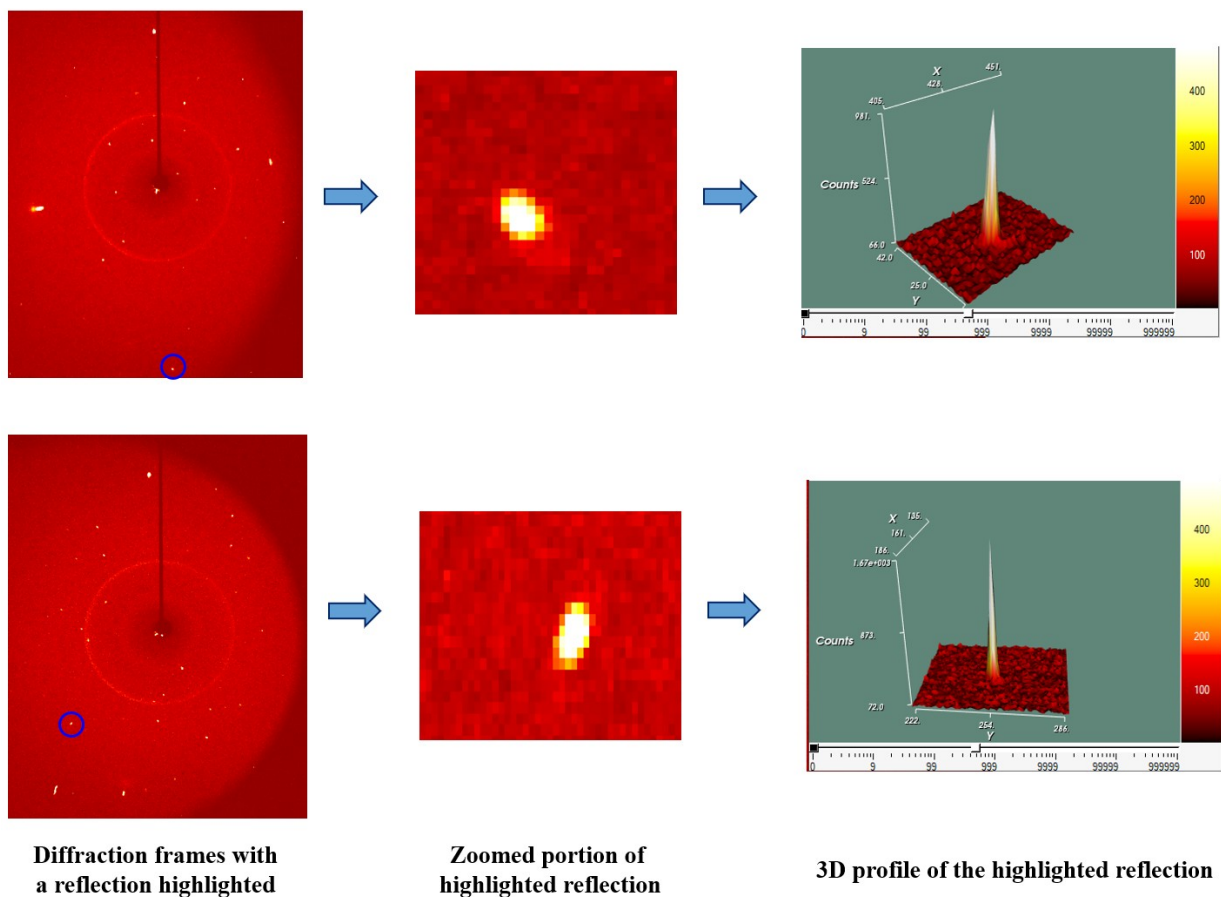
Figure SI-4   Selected diffraction frames and highlighted peaks with their 3D profile, which do not show any sign of peak splitting, indicating that reflections issued from both domains overlap each other.

$V_0 = 2711(20)$ Å³

$K_{T_0} = 6(2)$ GPa

$K'_{T_0} = 12(4)$ GPa

(a)

$V_0 = 2701(13)$ Å³

$K_{T_0} = 8(2)$ GPa

$K'_{T_0} = 9(5)$ GPa

(b)
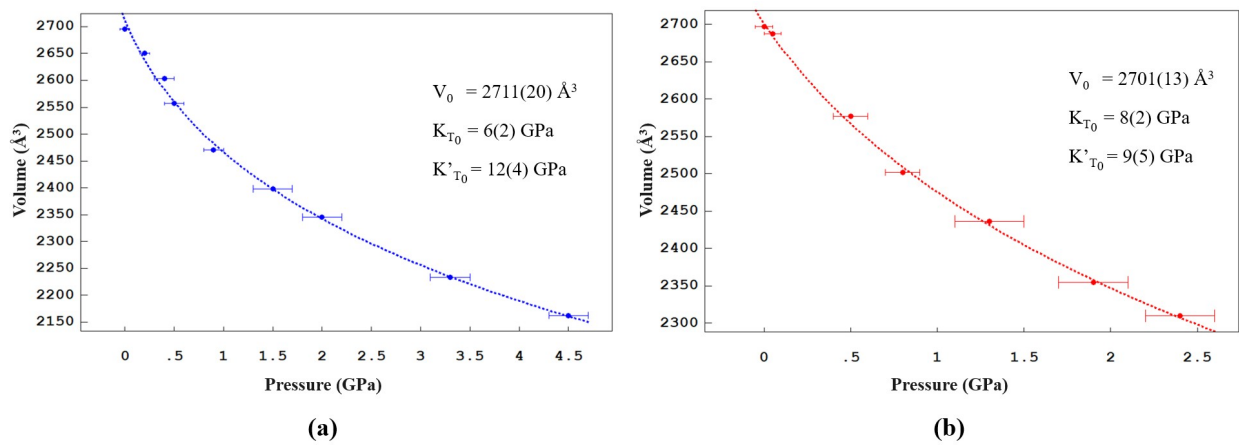
Figure SI-5   3rd order Birch-Murnaghan EOS fitting for (a) compression and (b) decompression experimental sub-data sets.
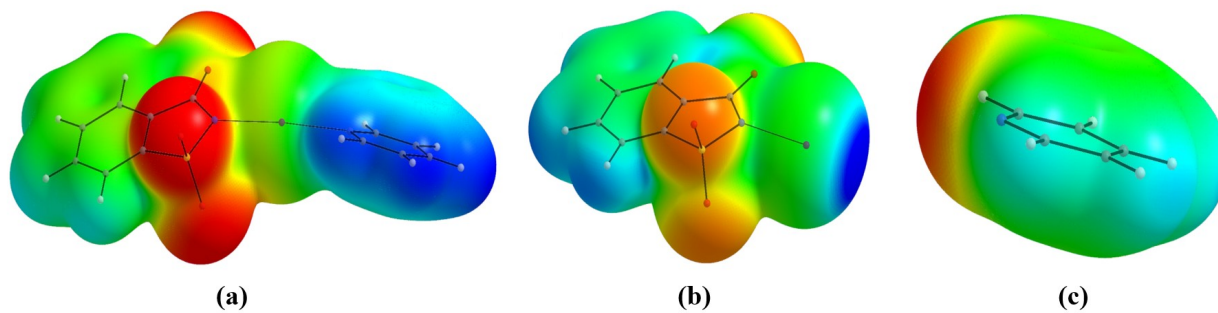
Figure SI-6   Electrostatic potential (ESP) maps drawn on the ρ = 0.002 a.u. isosurface for (a) *NISac·Py* adduct, (b) isolated *NISac* molecule, and (c) isolated *Py* molecule; all extracted from the experimental geometry at ambient conditions. ESP colouring: red = -0.07 a.u. to blue = +0.07 a.u. (B3LYP-D3/Def2-TZVP).
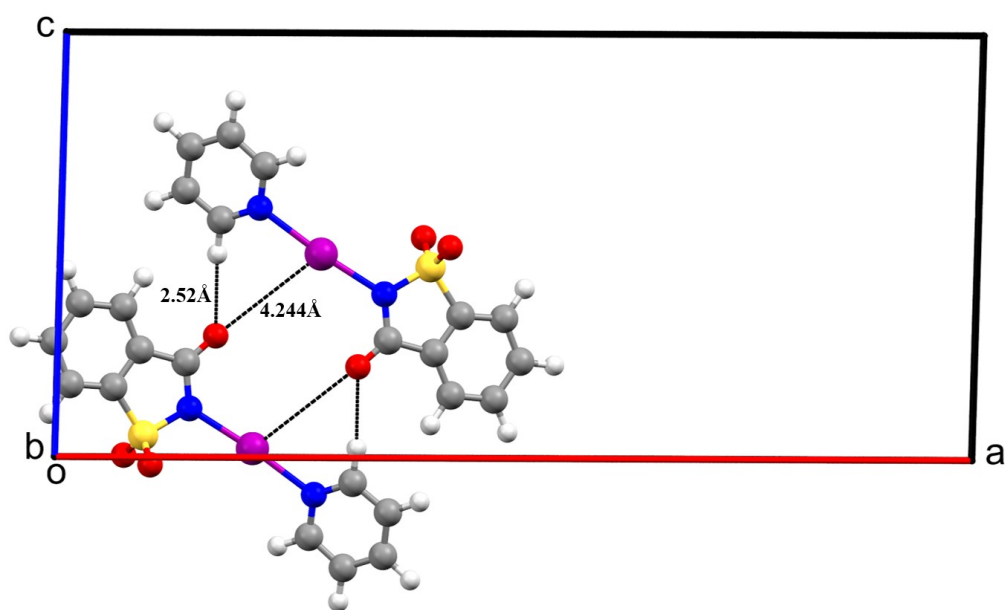

Figure SI-7   Interaction between *x,y,z* and 1/2-*x*,1-*y*,1/2-*z* adducts in the experimental *NISac·Py* crystal structure at ambient conditions. Characteristic distances are indicated as dashed lines and given in Å.
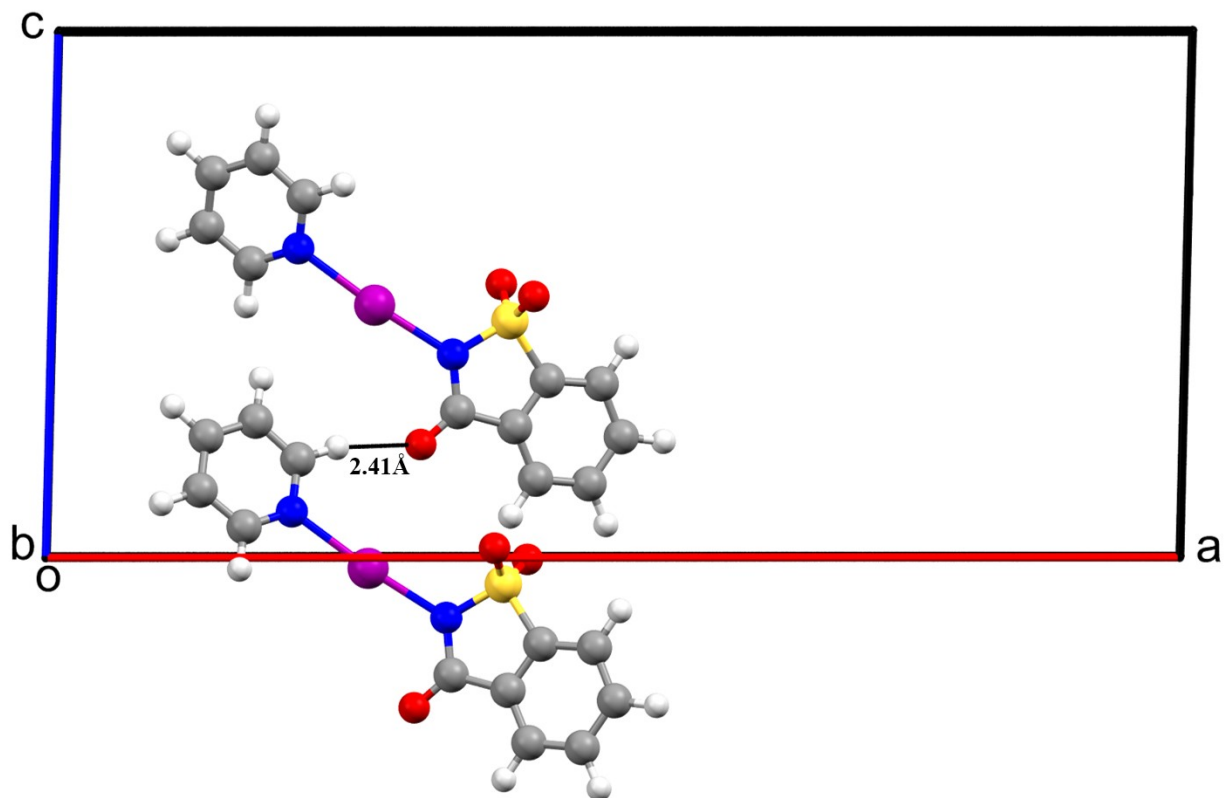
Figure SI-8   Interaction between *x,y,z* and *x*,1/2-*y*,-1/2+*z* adducts in the experimental *NISac·Py* crystal structure at ambient conditions.

Characteristic distances are indicated as dashed lines and given in Å.
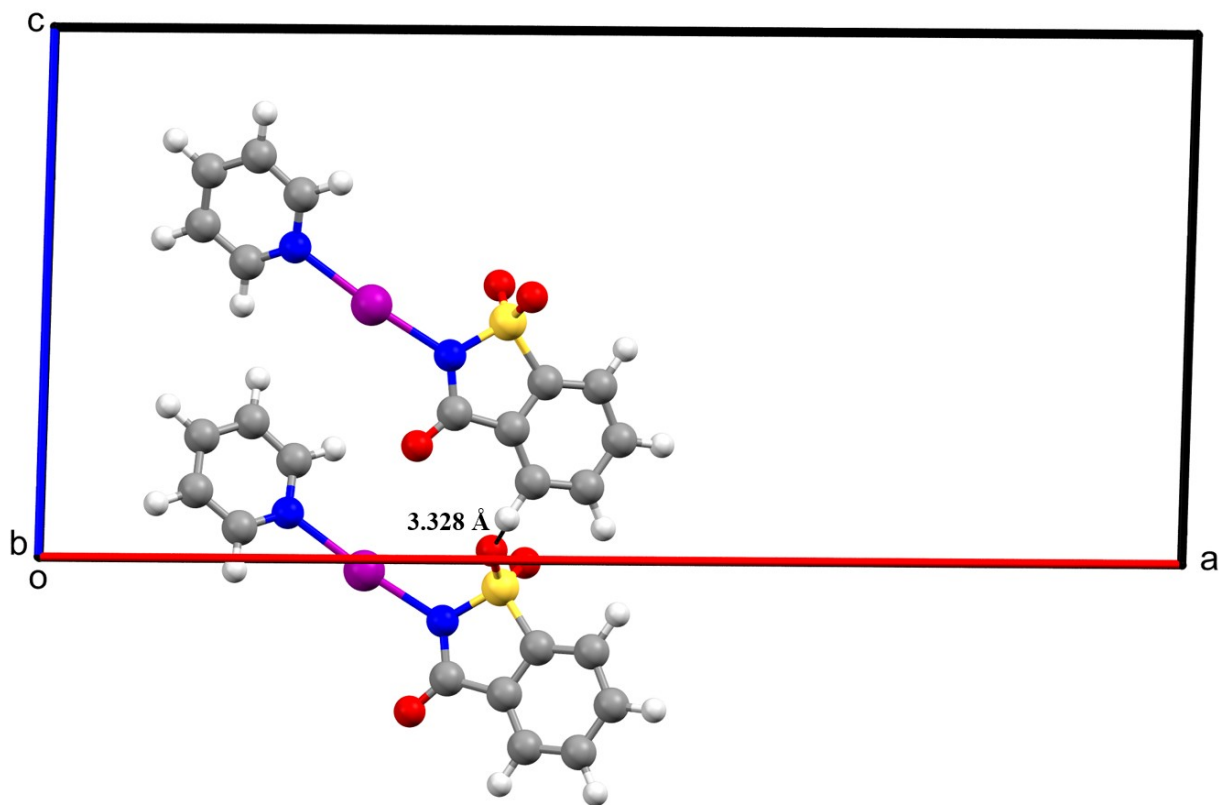
Figure SI-9   Interaction between *x,y,z* and *x*,1.5-*y*,-1/2+*z* adducts in the experimental *NISac·Py* crystal structure at ambient conditions.

Characteristic distances are indicated as dashed lines and given in Å.
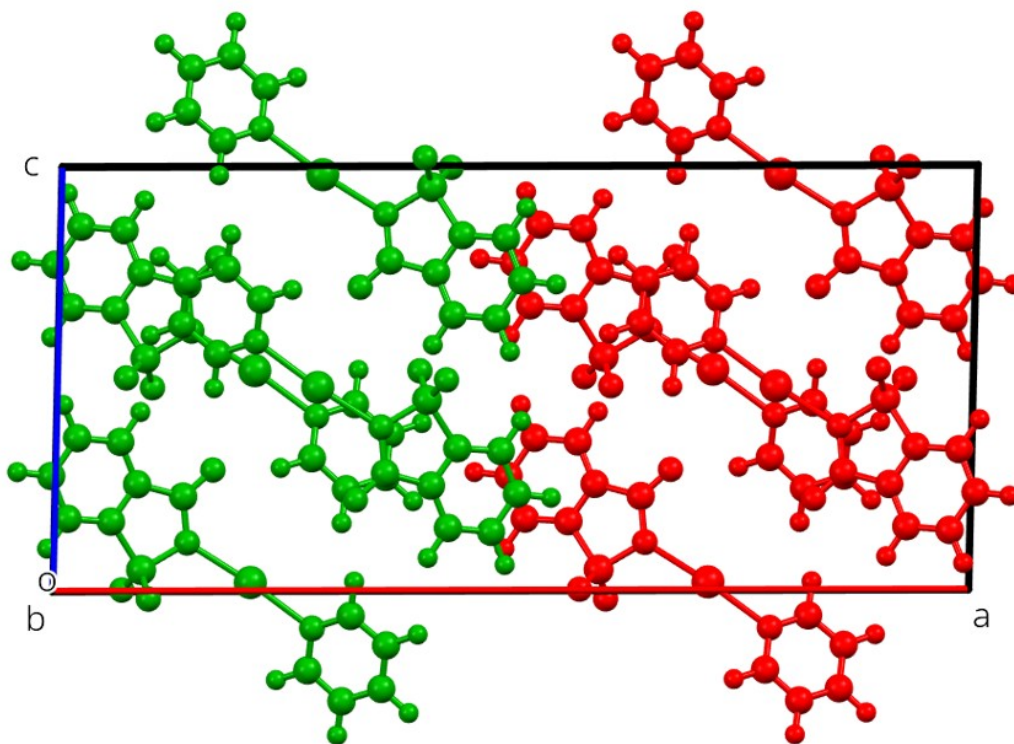
Figure SI-10   Molecular packing in the experimental *NISac·Py* crystal structure at at ambient conditions, highlighting the formation of (200) molecular planes whose cohesion is driven by the most intense interactions. Two such planes are depicted in green and red and interact through secondary less intense interactions.
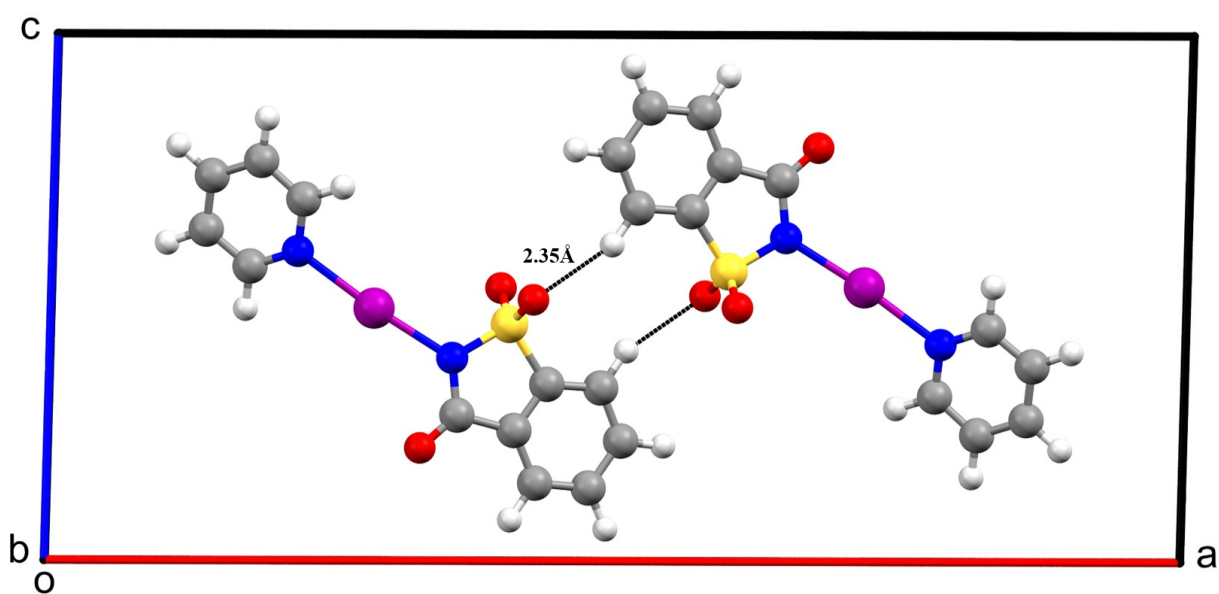
Figure SI-11   Interaction between x,y,z and 1-x,1-y,1-z adducts in the experimental *NISac·Py* crystal structure at ambient conditions. Characteristic distances are indicated as dashed lines and given in Å.
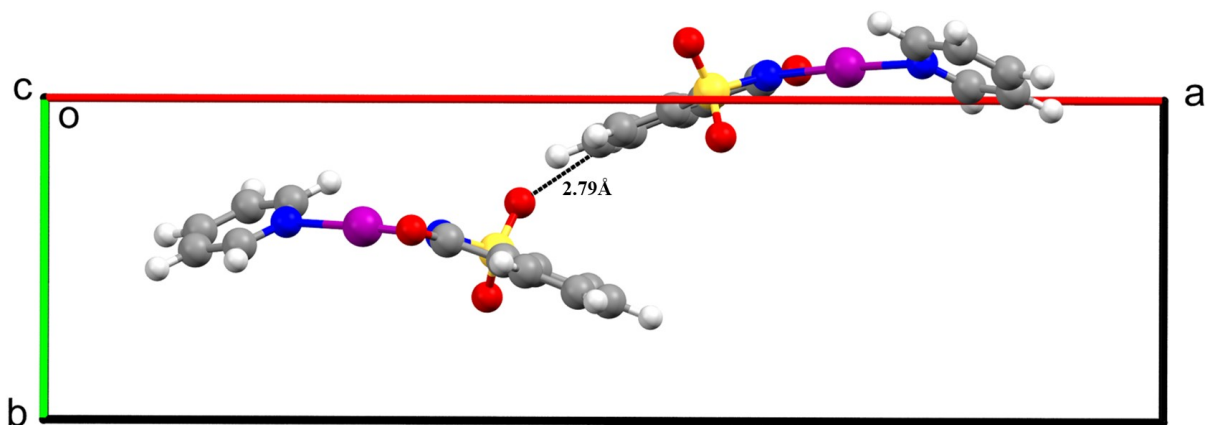
Figure SI-12   Interaction between x,y,z and 1-x,-1/2+y,1/2-z adducts in the experimental *NISac·Py* crystal structure at ambient conditions. Characteristic distances are indicated as dashed lines and given in Å.
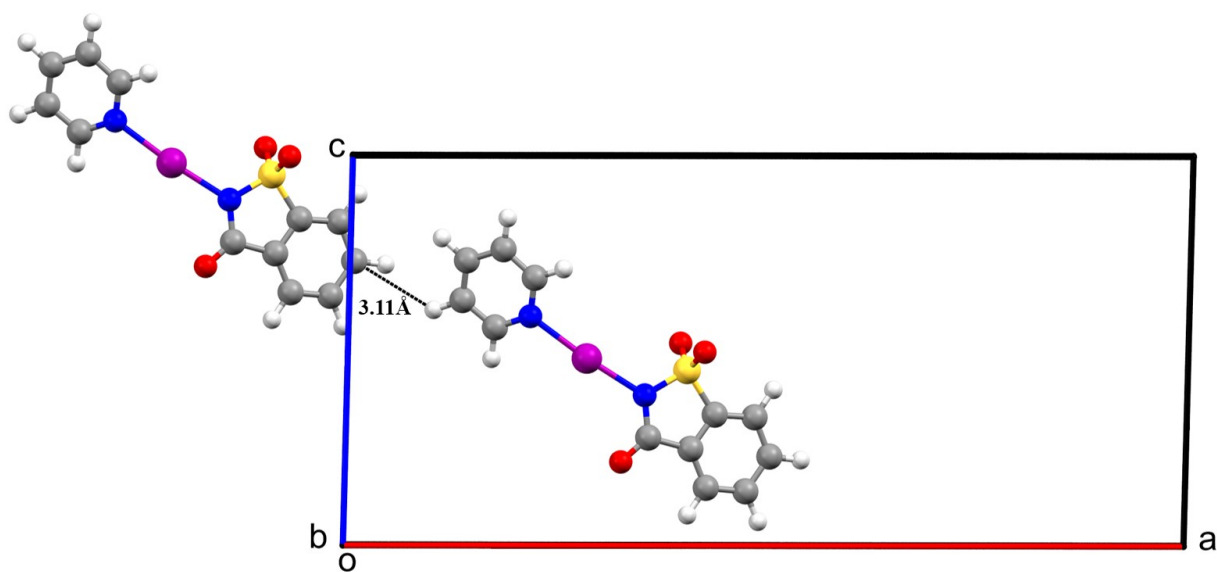

Figure SI-13   Interaction between x,y,z and -1/2+x,y,1/2+z adducts in the experimental *NISac·Py* crystal structure at ambient conditions. Characteristic distances are indicated as dashed lines and given in Å.
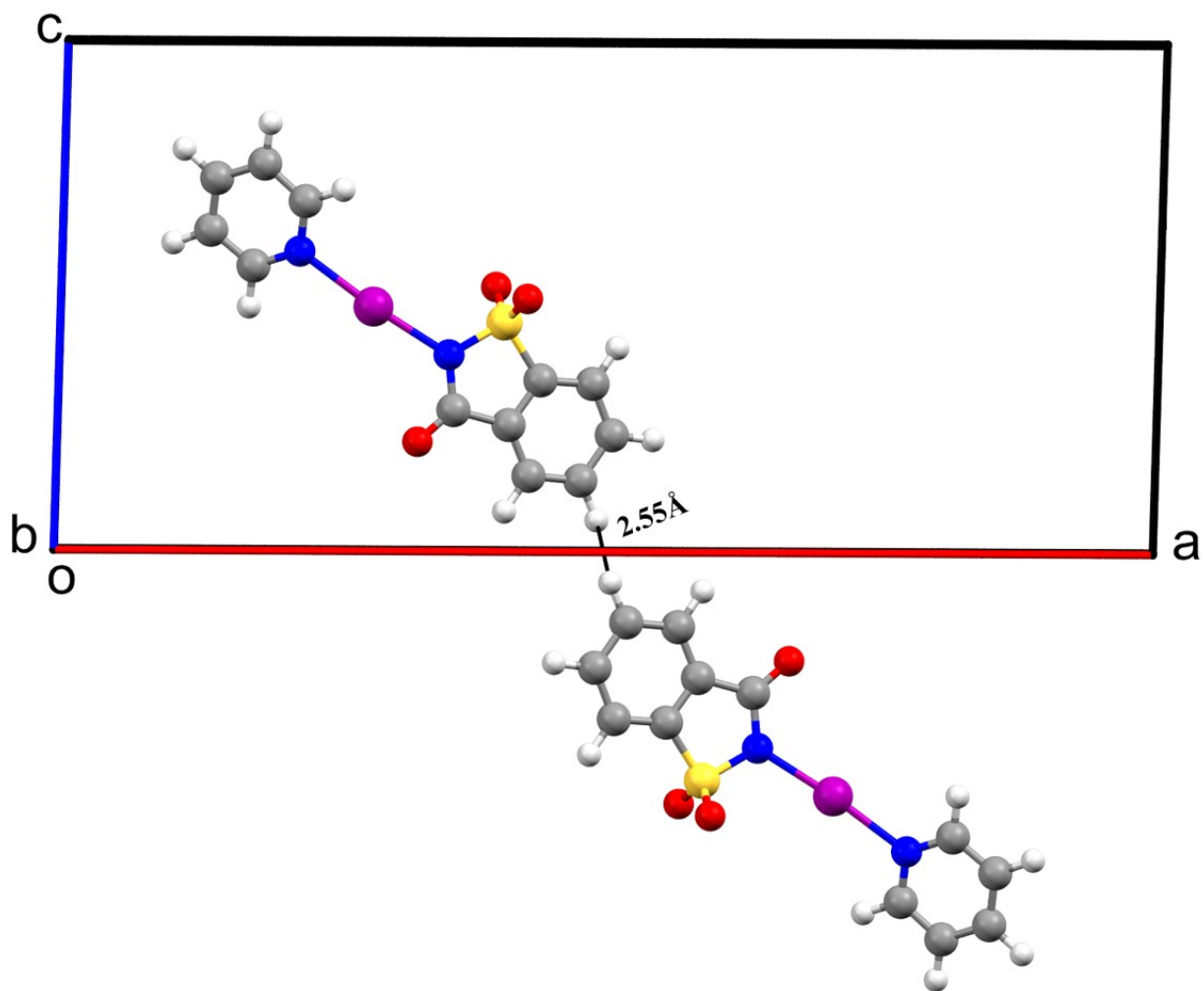
Figure SI-14 Interaction between x,y,z and 1-x,1-y,-z adducts in the experimental *NISac·Py* crystal structure at ambient conditions. Characteristic distances are indicated as dashed lines and given in Å.
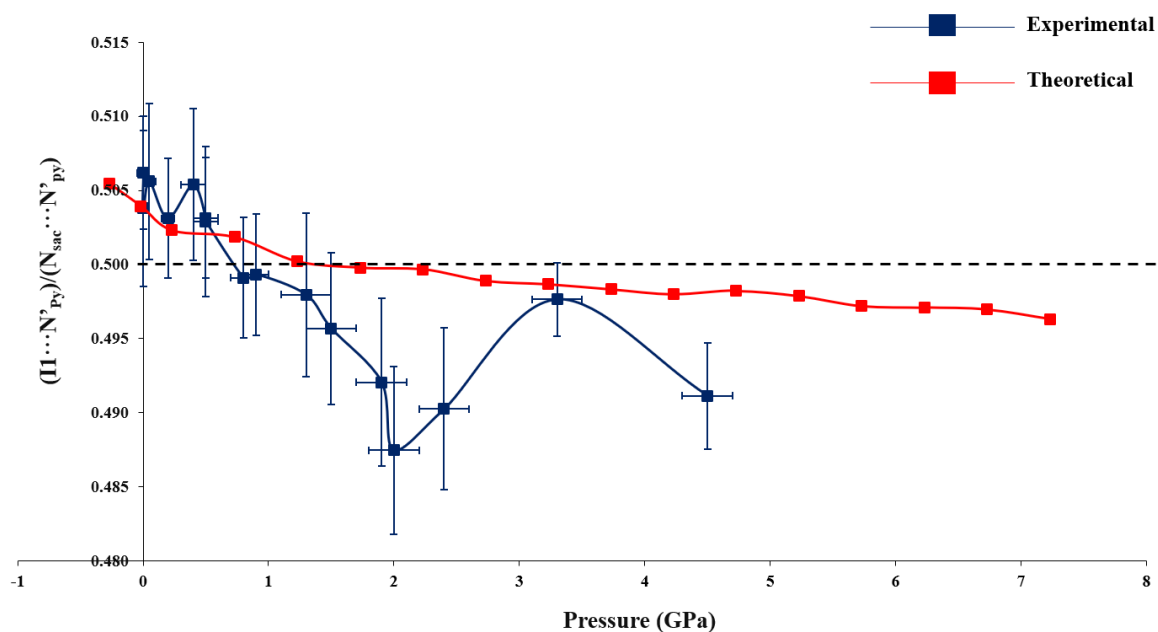
Figure SI-15   Variation of the normalized XB bonding distance $(I \cdots N'_{py})/(N_{sac} \cdots N'_{py})$ as a function of pressure. Curves connecting data are plotted for guiding eyes. Error bars are shown for experimental data.
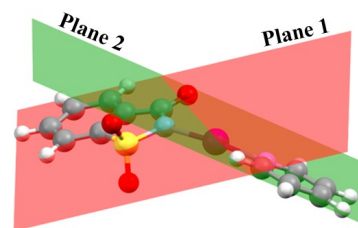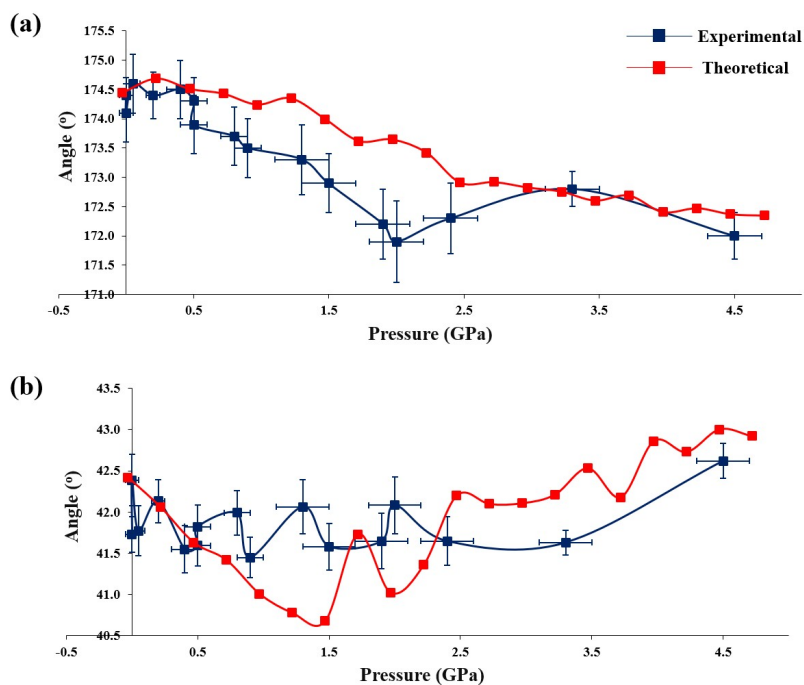

Figure SI-16   Variations as a function of pressure of: (a) $N_{sac}-I1 \cdots N'_{py}$ angle and (b) angle between molecular planes. Molecular planes are defined by the saccharine ring – Plane 1 (excluding iodine and hydrogen atoms) and the Pyridine ring – Plane 2 (excluding hydrogen atoms). They are denoted with red and green colours, respectively. Error bars are shown for experimental data. Lines connecting data are plotted for guiding eyes.
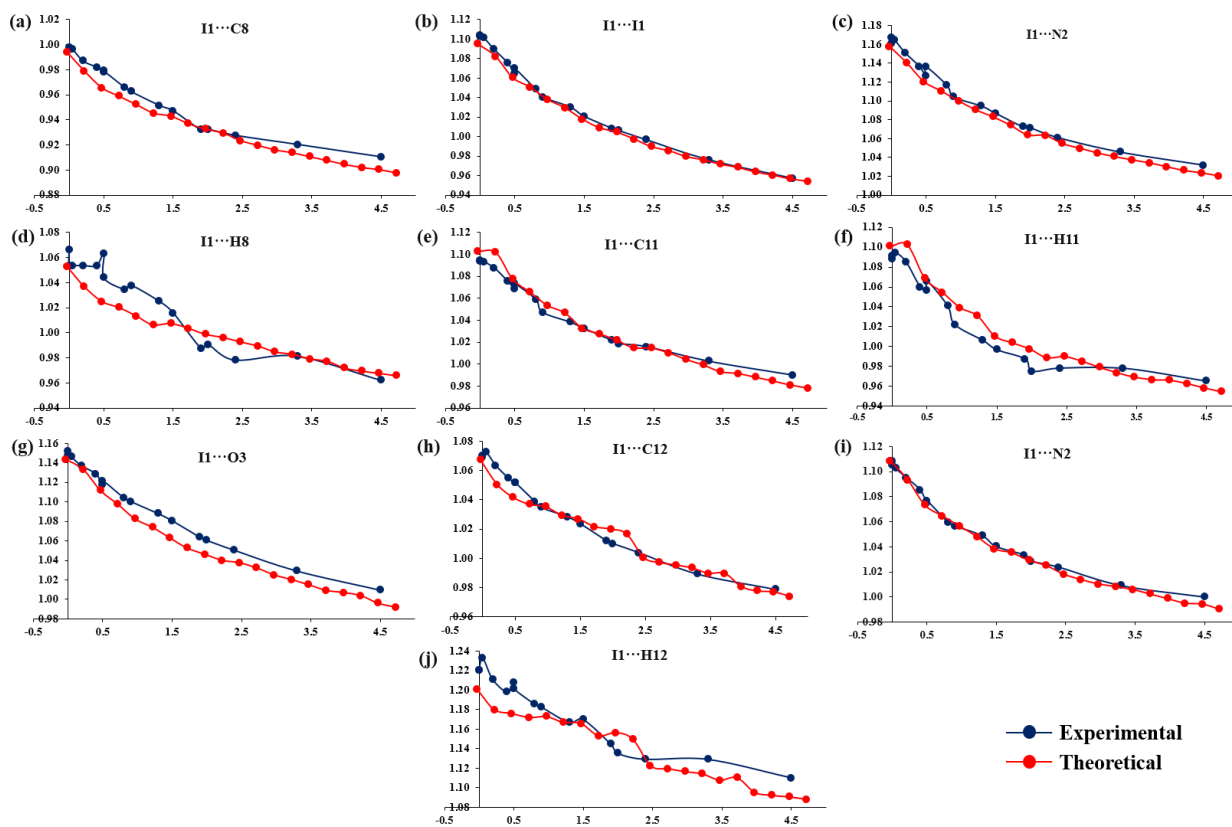
Figure SI-17 Variation of the Reduction Ratio (RR) calculated for intermolecular contacts involving I1(x,y,z) and atoms of neighbouring molecules, as a function of pressure. The neighbouring atom belong to (a)-(d) 1/2-x,-1/2+y,1-z, (e)-(f) 1/2-x,1-y,1.5-z, (g) x,1/2-y,1/2+z and (h)-(j) 1/2-x, 1/2+y,1-z, symmetry generated molecules.
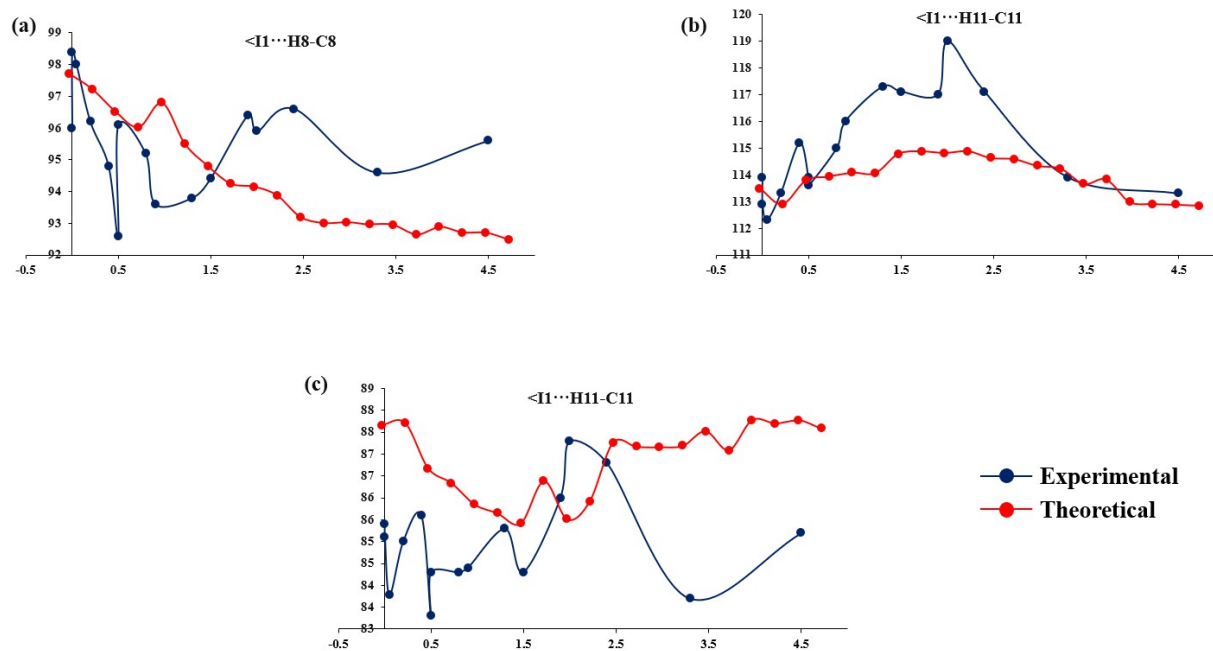
Figure SI-18   Variation of the HB angle involving I1(x,y,z) and atoms of neighbouring molecules, as a function of pressure. The HB acceptor belong to (a) 1/2-x,-1/2+y,1-z, (b) 1/2-x,1-y,1.5-z and (c) 1/2-x, 1/2+y,1-y, symmetry generated molecules.
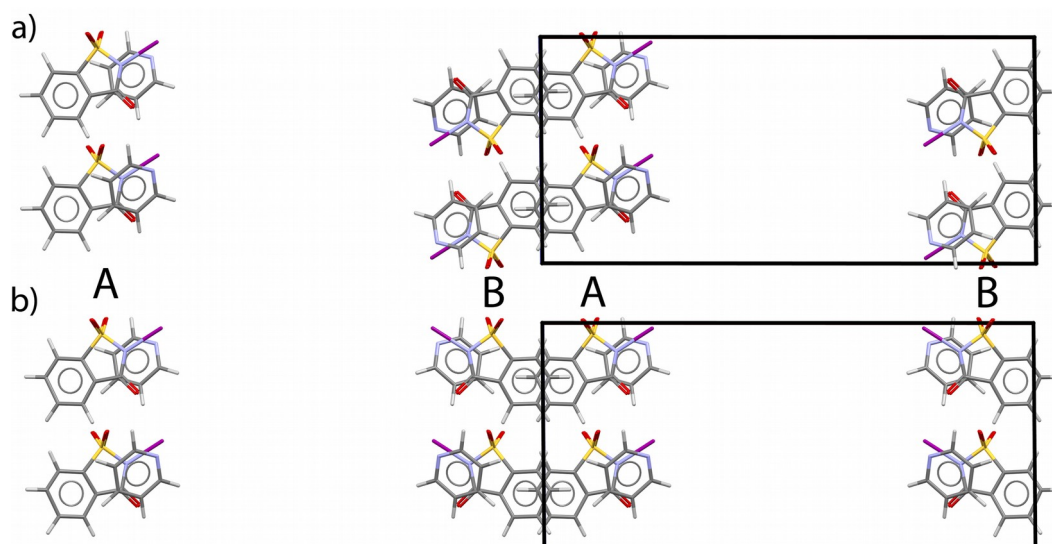

Figure SI-19   Structural models used to calculate the stabilization energy cost of the twining: a) Original (untwinned) *NISac·Py* structure with the central part of the unit cell omitted, described as sub-slabs A and B, b) Twin interface created by appropriate two-fold rotation of sub-slab B.

References

Dolenc, D. (2000). *Synlett* **2000**, 544-546.

Piermarini, G.J., Block, S., Barnett, J.D. and Forman, R.A. (1975). *J Appl. Phys*. **46**, 2774-2780.

Voute, A., Deutsch, M., Kalinko, A., Alabarse, F., Brubach, J.-B., Capitani, F., Chapuis, M., Ta Phuoc, V., Sopracase, R. and Roy, P. (2016). *Vibr. Spectr*. **86**, 17-23.